https://mathco.journals.pnu.ac.ir

Payame Noor University

Control and Optimization in Applied Mathematics

Volume 11, Issue 2, Summer-Autumn 2026, Pages 179–199

DOI:10.30473/coam.2026.75815.1338

OPEN ACCESS

Control and Optimization in Applied Mathematics

Research Article

Numerical Solution of Homogeneous Aw-Rascle Type Traffic Flow Models Using an Improved Wave Propagation-HLLE Approach

Alireza Ezzati[1] **Mahdi Mollazadeh**[1] **Sadegh Moodi**[2] **Morteza Araghi**[1] ✉ **Hossein Mahdizadeh**[1]

[1]Department of Civil Engineering, Faculty of Engineering, University of Birjand, Iran

[2]Department of Civil Engineering, Faculty of Mining, Civil and Chemical Engineering, Birjand University of Technology, Birjand, Iran

Article History

Received: September 17, 2025

Accepted: March 9, 2026

Available online: May 21, 2026

Abstract. Homogeneous second-order Aw-Rascle-type models have demonstrated greater effectiveness than their non-homogeneous counterparts in traffic flow modeling. This study addresses the numerical solution of hyperbolic conservation laws governing these models by coupling the second-order HLLE Riemann solver, a Godunov-type finite volume approach, with the wave propagation algorithm. A novel wave-speed selection strategy is proposed by comparing characteristic velocities with Roe speeds, yielding solutions with guaranteed positive density and speed. The proposed IWP-HLLE method is applied to simulate shock, rarefaction, and contact discontinuity waves under homogeneous long-road conditions, eliminating the influence of external source terms and ensuring the homogeneity of the governing hyperbolic equations. Its performance is benchmarked against the MacCormack scheme supplemented by two standard stabilization techniques, namely artificial viscosity (AV) and central differencing (CD). Spatiotemporal distributions and density profiles are examined across four representative traffic scenarios: free flow, congested traffic flow, queue dissolution, and congested flow with non-equilibrium velocity and uniform density. The results demonstrate that the IWP-HLLE approach substantially suppresses numerical oscillations compared to both AV and CD methods while maintaining stability across all test cases.

Keywords. Aw-Rascle-Zhang model, Finite volume method, HLLE Riemann solver, IWP-HLLE approach, Wave propagation algorithm.

MSC. 65M08; 90B20.

How to Cite

Ezzati, A.R., Mollazadeh, M., Moodi, S., Araghi, M., Mahdizadeh, H. (2026). "Numerical solution of homogeneous Aw-Rascle type traffic flow models using an improved wave propagation-HLLE approach". *Control and Optimization in Applied Mathematics*, 11(2), 179-199. https://doi.org/10.30473/coam.2026.75815.1338

✉Corresponding author. **E-mail:** m.araghi@birjand.ac.ir

1 Introduction

Urban communities face severe traffic congestion due to the ever-increasing number of vehicles. Efficient traffic control and management are crucial to resolving this matter [14]. However, human behavior and sudden changes in road geometry caused by accidents and weather conditions make traffic systems inherently dynamic and unpredictable [4]. Over the years, various techniques have been developed to forecast traffic conditions [6]. Among these, continuous approaches based on mathematical modeling have proven to be among the most effective tools for traffic flow analysis [16]. Continuous Traffic Flow Modeling (CTFM) treats traffic as a fluid-like medium, enabling the use of well-established conservation principles. While first-order models assume that local speed instantaneously equilibrates with local density, second-order models define the local speed through a momentum equation [20]. This added complexity allows second-order CTFM to analyze traffic shocks under equilibrium conditions and to incorporate acceleration behavior, driver reaction time, and anticipation effects into the governing equations. A key advantage of second-order models is their ability to capture nonlinear traffic phenomena that lie beyond the descriptive capability of first-order formulations [20]. Nevertheless, the mathematical complexity of these models necessitates the use of advanced numerical methods [22].

Second-order CTFM is mathematically classified as a nonlinear system of hyperbolic partial differential equations (PDEs). When a source term is present, the system is categorized as non-homogeneous; representative examples include the Payne–Whitham [17], Kerner–Konhäuser [8], and gas-kinetic-based models. In contrast, models such as the Aw–Rascle (AR) [24] and Aw–Rascle–Zhang (ARZ) [10] are classified as homogeneous due to the absence of source terms. A well-known deficiency of many non-homogeneous models is their failure to preserve the anisotropic property of traffic flow, leading to unrealistic oscillatory behavior at traffic discontinuities. This shortcoming is effectively addressed by the AR and ARZ models [2]. Since the continuity and momentum equations of these second-order models do not admit closed-form analytical solutions, numerical methods are indispensable [14]. Among the most widely adopted approaches in CTFM is the finite volume method, which is grounded in the integral form of physical conservation laws and is naturally suited to handling discontinuous solutions. Explicit finite volume schemes based on the wave propagation algorithm [13] belong to the class of Godunov-type methods and are particularly effective for shock capturing, providing non-oscillatory results in the presence of flow discontinuities.

Wave propagation speeds in the Riemann problem are generally computed using either exact or approximate solvers. The exact Riemann solver [11] determines wave speeds from analytical solutions and is highly accurate; however, its practical applicability is severely limited by the absence of closed-form solutions for the nonlinear PDEs governing traffic flow. Consequently, approximate solvers—including Roe, HLL, HLLE, HLLC, and various hybrid formulations—have become standard in practical implementations [11, 14]. These methods differ primarily in their discretization strategies with respect to wave directionality and propagation speed [13, 11]. High-order spatial discretization schemes such as MUSCL, CBTOU, WENO-JS, and WENO-Z can reduce numerical diffusion and sharpen wave front resolution, but they frequently generate spurious oscillations near intermediate states where contact discontinuities and rarefaction waves interact.

This limitation is thoroughly documented in the work of Mohammadian et al. [15], who systematically evaluated the performance of the Rusanov, HLL, and HLLC approximate Riemann solvers for the ARZ model across the full solution range from free-flow to congested traffic. Their study coupled these solvers with several spatiotemporal discretization schemes—including Euler-Upwind, second-order MINMOD and MUSCL, the cell-based third-order upwind (CBTOU) approach, and the fifth-order WENO-JS and WENO-Z schemes— combined with a third-order TVD Runge–Kutta method for temporal integration. At low resolution, all solvers successfully captured the qualitative wave structure of the Riemann solutions, though the results exhibited excessive diffusion near contact discontinuities. At high resolution, the behavior varied considerably across scheme combinations. Notably, while the pairing of MUSCL or WENO-type reconstructions with the HLL solver reduced numerical diffusion

most effectively, it simultaneously introduced oscillatory behavior near intermediate states. The persistence of spurious oscillations even in high-order schemes suggests that the root cause lies in the inherent non-convexity and nonlinearity of models such as the ARZ model—implying that solver selection alone is insufficient, and that complementary stabilization tools such as flux limiters or regularization techniques are essential to prevent unphysical solution behavior.

In a related study, Araghi et al. [2] developed a modified wave propagation algorithm for four macroscopic traffic flow models: Payne–Whitham [17], AR [24], ARZ [10], and Khan et al. [9]. Their scheme employed characteristic wave speeds to evaluate right- and left-going fluctuations, and its performance was benchmarked against fifth-order WENO, second-order MUSCL, and the Roe decomposition technique. Although the scheme exhibited overall stability and reduced diffusion, it produced strong spurious oscillations at the interaction of contact discontinuity and rarefaction waves, and yielded non-physical negative densities and velocities in both AR and ARZ models. This finding exposes a critical gap: even hybrid combinations of approximate Riemann solvers and high-order reconstruction schemes may fail to preserve physical admissibility under extreme flow conditions. More recently, Rastegar Moghadam Najafzadeh et al. [18] introduced the IFW-HLLE method—a hybrid approach combining characteristic and Roe velocities—to solve two non-homogeneous second-order macroscopic traffic flow models. This work underscores a growing trend toward adaptive hybrid schemes that dynamically balance accuracy and stability based on the local wave structure.

To overcome these limitations, the present study proposes a novel wave-speed selection strategy that blends characteristic and Roe-type velocities within a Godunov-type finite volume framework for homogeneous second-order traffic flow models. This hybrid strategy ensures the preservation of physical positivity constraints, enhances numerical stability, and substantially reduces spurious oscillations near discontinuities. The improvement is realized by embedding the HLLE approximate Riemann solver into an enhanced wave propagation algorithm, augmented by the Monotonized Central (MC) limiter [11] to enforce monotonicity and suppress unphysical overshoots. The resulting scheme is designated the Improved Wave Propagation HLLE (IWP-HLLE) method. Its advantages are most pronounced in scenarios involving sharp density gradients or mixed wave interactions, as demonstrated through the numerical experiments presented in this study. General formulations of the IWP-HLLE are derived for both the AR and ARZ models. Performance is assessed through four representative traffic scenarios, each designed to isolate distinct wave interaction regimes: the first three cases involve non-equilibrium density distributions with uniform velocity, while the fourth considers uniform density with non-equilibrium velocity. The IWP-HLLE results are systematically compared against the standard MacCormack finite-difference scheme augmented by artificial viscosity (AV) and central differencing (CD) smoothing, with the aim of demonstrating improvements in oscillation suppression, stability, and convergence behavior.

The remainder of this paper is organized as follows. Section 2 presents the governing equations of the homogeneous AR and ARZ second-order traffic flow models, followed by a detailed derivation of the IWP-HLLE formulation. Section 3 describes the road geometry and the numerical stability criterion employed. The four benchmark test cases are solved and analyzed in Section 4, where the performance of IWP-HLLE is compared against the MacCormack-AV and MacCormack-CD schemes through spatiotemporal density profiles and RMSE metrics. Finally, Section 5 summarizes the principal findings and identifies directions for future research, including the extension of the proposed framework to two-dimensional traffic networks.

2 Material and Methods

2.1 Homogeneous Second-Order Traffic Flow Models

The conservation laws of one-dimensional quasi-linear and nonlinear hyperbolic systems can generally be represented as follows [11]:

$$\mathbf{U}_t + F(\mathbf{U})_x = 0. \tag{1}$$

The vector U comprises unknowns or conserved variables, while $F(U)$ denotes the flux gradient in the x direction. Equation (1) is a prevalent representation of homogeneous hyperbolic systems, encompassing second-order traffic flow models like the Aw-Rascle model. The quasi-linear form of Equation (1) can be expressed as follows [11]:

$$\mathbf{U}_t + F'(\mathbf{U})\,\mathbf{U}_x = 0. \tag{2}$$

The Jacobian matrix for the flux gradient term is denoted by $F'(U)$. The eigenvalues (represented by λ), which correspond to the characteristic speeds of the system, can be calculated by solving the following equation [11]:

$$|F'(\mathbf{U}) - \lambda\,\mathrm{I}\,| = 0. \tag{3}$$

A system is classified as hyperbolic if Equation (3) has real eigenvalues [5]. If λ is an eigenvalue of $F'(U)$, it implies the existence of a non-zero vector x satisfying the following equation [11]:

$$F'(\mathbf{U})\,.\mathrm{r} = \lambda.\mathrm{r}. \tag{4}$$

The vector r is called the eigenvector of $F'(U)$.

2.2 The AR Model

The Aw-Rascle model [3] is a well-established second-order macroscopic traffic flow model that describes traffic as a compressible fluid-like medium, drawing conceptual analogies to gas dynamics [21]. The mathematical formulation of the Aw-Rascle model is as follows:

$$\begin{gathered}\rho_{\mathrm{t}}+(\rho\mathrm{u})_{\mathrm{x}}=0,\\ (\rho(\mathrm{u}+\mathrm{P}(\rho)))_{\mathrm{t}}+(\rho\mathrm{u}(\mathrm{u}+\mathrm{P}(\rho)))_{\mathrm{x}}=0,\\ \mathrm{P}(\rho)=C_0^2\rho^{\gamma}-\psi,\end{gathered} \tag{5}$$

where ρ denotes vehicle density (vehicles per meter), u is the macroscopic velocity (meters per second), and $P(\rho)$ is the traffic pressure function, representing the collective response of drivers to upstream density variations. All pressure functions must satisfy compatibility conditions with respect to velocity and density gradients; the negative sign reflects the inverse relationship between density increase and vehicle acceleration. The constants C_0, γ, and ψ are model parameters governing the pressure–density relationship and driver response at the macroscopic scale [12, 13, 19]. The constants γ and ψ are used for pressure adjustment.

2.3 The ARZ Model

The ARZ model [23] differs from the AR model solely in the definition of the traffic pressure function, which is given by:

$$\mathrm{P}(\rho) - \mathrm{V_e}(\rho) = -\mathrm{u_m}(1-\frac{\rho}{\rho_\mathrm{m}}), \tag{6}$$

where $\mathrm{V_e}(\rho)$ represents the equilibrium velocity, ρ_m is the maximum density, and $\mathrm{u_m}$ denotes the maximum speed on the road. In the ARZ model, the acceleration equation is derived based on a microscopic model, leading to a better representation of the non-isotropic properties of traffic flow.

2.4 The IWP-HLLE Method

The IWP-HLLE approach is built upon Godunov's finite volume method, also known as the wave propagation algorithm, which requires solving the Riemann problem [11] at each cell interface and time step to evaluate the numerical flux. The wave propagation algorithm is generally written in the following form [11]:

$$U_i^{n+1} = U_i^n - \frac{\Delta t}{\Delta x}\left(A^+\Delta U_{i-1/2} + A^-\Delta U_{i+1/2}\right) - \frac{\Delta t}{\Delta x}\left(\widetilde{F}_{i+1/2} - \widetilde{F}_{i-1/2}\right). \tag{7}$$

In which $A^\pm\Delta U_{i\pm1/2}$ indicates the right- and left-going fluctuations achieved from the Riemann problem solving. The second-order accuracy is represented by the term $\widetilde{F}_{i\pm1/2}$ and is defined as follows [11]:

$$\widetilde{F}_{i-1/2} = \frac{1}{2}\sum_{k=1}^{m}\left(I - \frac{\Delta t}{\Delta x}\left|\lambda_K\right|\right)\left|\lambda_K\right|\widetilde{W}_{k,i-1/2}. \tag{8}$$

It is assumed that a rarefaction wave corresponds to the k-th characteristic field of the problem. In addition, the W_k wave travels at the λ_k velocity in the cell interface, and $\widetilde{W}_{K,i-1/2} = \varphi(\theta)\, W_{k,i-1/2}$ is used to represent the limited Riemann wave. The Monotonized Centre (MC) is selected here as the limiter function $(\varphi(\theta)$ to avoid unphysical fluctuations near discontinuities [11]:

$$\begin{aligned}\varphi(\theta) &= \max\left(\min(2,\theta), \min(1,2\theta), 0\right),\\ \theta_{i-1/2}^n &= \frac{(W_{k,I-1/2}W_{k,i-1/2})}{(W_{k,i-1/2}W_{k,i-1/2})},\end{aligned} \tag{9}$$

where θ is a scalar coefficient.

Therefore, the general formulation of the IWP-HLLE approach for homogeneous AR and ARZ models is written as below:

$$\begin{bmatrix} U_i - U_{i-1} \\ F(U_i) - F(U_{i-1}) \end{bmatrix} = \sum_{k=1}^{2M_W}\begin{bmatrix} W_{k,i-1/2} \\ \xi_{k,i-1/2} \end{bmatrix}. \tag{10}$$

The HLLE method [7] determines wave speeds by comparing the characteristic velocities and the Roe speeds. These wave speeds for the homogeneous AR model can be written as follows:

$$\begin{aligned}s_{1,i-1/2} &= min\left(u_{i-1} - C_0^2\gamma\rho^\gamma, \widetilde{u}_{i-1/2} - C_0^2\gamma\widetilde{\rho}_{i-1/2}\right),\\ s_{2,i-1/2} &= \max\left(u_i, \widetilde{u}_{i-1/2}\right).\end{aligned} \tag{11}$$

This wave-speed selection ensures that the flux evaluation remains consistent with the underlying wave structure of the AR and ARZ models. In addition, the approximate density and velocity are obtained as below [1]:

$$\begin{aligned}\widetilde{\rho}_{i-1/2} &= \sqrt{\rho_i\rho_{i-1}},\\ \widetilde{u}_{i-1/2} &= \frac{\sqrt{\rho_{i-1}}\widetilde{u}_{i-1} + \sqrt{\rho_i}\widetilde{u}_i}{\sqrt{\rho_{i-1}} + \sqrt{\rho_i}}.\end{aligned} \tag{12}$$

Therefore, Equation (10) is re-written in the following form using the HLLE wave speeds in the IWP-HLLE approach:

$$\begin{bmatrix} 1 & 1 \\ (\widetilde{u}_i - C_0^2\gamma\rho_i{}^\gamma) & \widetilde{u}_i \end{bmatrix} \begin{bmatrix} \beta_1 \\ \beta_2 \end{bmatrix} = \begin{bmatrix} \rho_i\widetilde{u}_i - \rho_{i-1}\widetilde{u}_{i-1} \\ \rho_i\widetilde{u}_i(\widetilde{u}_i + C_0^2\gamma\rho_i^\gamma) - \rho_{i-1}\widetilde{u}_{i-1}(\widetilde{u}_{i-1} + C_0^2\gamma\rho_{i-1}^\gamma \end{bmatrix}. \tag{13}$$

By solving the linear system of Equation (13), the coefficients β_1 and β_2 are calculated as follows for the AR model:

$$\beta_1 = \frac{(\rho_i\widetilde{u}_i(\widetilde{u}_i - C_0^2\gamma\rho^\gamma) - \rho_{i-1}\widetilde{u}_{i-1}(\widetilde{u}_i - C_0^2\gamma\rho^\gamma)}{(\widetilde{u}_i - C_0^2\gamma\rho^\gamma) + \widetilde{u}_i} - \frac{(\rho_i\widetilde{u}_i - \rho_{i-1}\widetilde{u}_{i-1})\left(\widetilde{u}_i - C_0^2\gamma\rho^\gamma\right)}{(\widetilde{u}_i - C_0^2\gamma\rho^\gamma) + \widetilde{u}_i}, \tag{14}$$

$$\beta_2 = (\rho_i\widetilde{u} - \rho_{i-1}\widetilde{u}_{i-1}) - \beta_1.$$

These coefficients are calculated in a similar way for the ARZ model as below:

$$\beta_1 = \frac{(\chi + \rho_i v_e(\rho_i))\left(\widetilde{u}_i - \rho\frac{\widetilde{u}_i}{\rho_i}\right)}{\left(\widetilde{u}_i - \rho\frac{\widetilde{u}_i}{\rho_i}\right) + \widetilde{u}_i} - \frac{(\chi + \rho_{i-1}v_e(\rho_{i-1}))\left(\widetilde{u}_{i-1} - \rho\frac{\widetilde{u}_{i-1}}{\rho_{i-1}}\right)}{\left(\widetilde{u}_i - \rho\frac{\widetilde{u}_i}{\rho_i}\right) + \widetilde{u}_i}$$

$$- \frac{((\chi + \rho_i v_e(\rho_i)) - (\chi + \rho_{i-1}v_e(\rho_{i-1})))\left(\widetilde{u}_{i-1} - \rho\frac{\widetilde{u}_{i-1}}{\rho_{i-1}}\right)}{\left(\widetilde{u}_i - \rho\frac{\widetilde{u}_i}{\rho_i}\right) + \widetilde{u}_i}, \tag{15}$$

$$\beta_2 = ((\chi + \rho_i v_e(\rho_i)) - (\chi + \rho_{i-1}v_e(\rho_{i-1})) - \beta_1.$$

In Equation 15, the values of χ represent the differences between the actual flow $q = \rho u$ and the equilibrium flow $q_e = \rho v_e$.

The IWP-HLLE formulation effectively preserves the positivity of density and velocity while significantly suppressing numerical diffusion. When combined with the MC limiter, the proposed approach successfully mitigates spurious oscillations near contact discontinuities. Nevertheless, minor residual fluctuations may persist in highly non-equilibrium regimes—though these remain substantially smaller than those observed in alternative methods.

2.5 Comparison with Existing Flux-Wave HLLE Methods

The present study computes shock, rarefaction, and contact discontinuity wave speeds for homogeneous Aw–Rascle-type models spanning the full solution range from free-flow to congested traffic. This distinguishes the current work from Rastegar Moghadam Najafzadeh et al. [18], who developed the IFW-HLLE algorithm for two non-homogeneous Payne–Whitham (PW)-type models that include a relaxation-based source term.

Second-order continuum models containing a source term are classified as non-homogeneous. In contrast, the AR and ARZ models lack source terms and are therefore homogeneous. A further distinction is that many non-homogeneous models violate the anisotropy condition—implying that drivers respond to vehicles behind them—whereas homogeneous models such as AR and ARZ inherently satisfy anisotropy and possess proven solution existence for key initial value problems.

The present work applies the ARZ model to a realistic 12 km road segment across four distinct scenarios, whereas the study in [18] was confined to a 100 m circular road, limiting generalizability to real-world conditions.

3 Geometry and Stability Condition

The simulations are conducted on a homogeneous, open long-road segment without on-ramps or off-ramps, so as to isolate the hyperbolic wave dynamics from external source effects. The road length is set to $L = 12{,}000$ m, providing a sufficient spatial domain for tracking long-term traffic wave evolution [2].

The Courant–Friedrichs–Lewy (CFL) stability condition [13] governs the admissible time step for the explicit wave propagation algorithm. For the one-dimensional scheme, this condition requires:

$$\mathrm{Cr} = \frac{(\max\ s_{k,i-1/2})\,\Delta t}{\Delta x} < 1, \tag{16}$$

where Δt and Δx denote the time step and spatial cell width, respectively.

4 Results and Discussion

This section evaluates the performance of the IWP-HLLE approach in solving both the AR and ARZ models. A mesh-refinement study with smooth initial conditions is first conducted to assess convergence: the results confirm second-order accuracy in smooth regions and first-order accuracy near shocks and contact discontinuities. The IWP-HLLE results are then systematically compared against the MacCormack finite-difference scheme [16], a predictor–corrector method widely used for second-order hyperbolic PDEs, augmented by two stabilization techniques: Artificial Viscosity (AV) and Central Differencing (CD) smoothing.

Mohammadian and van Wageningen-Kessels [16] utilized this method to solve the homogeneous AR and ARZ models by employing two smoothing methods, i.e., Artificial Viscosity (AV) and Central Dispersion (CD). The main equations involved are as follows:

• Artificial Viscosity

$$U_i^{n+1} = (1-S)\,.U_i^{n+1} + S\left(\frac{U_i^{n+1} - U_{i-1}^{n+1}}{2}\right). \tag{17}$$

• Central Dispersion

$$U_i^{n+1} = U_i^{n+1} + \varphi_{i+1/2}(U_{i+1}^{n+1} - U_i^{n+1}) - \varphi_{i-1/2}(U_i^{n+1} - U_{i-1}^{n+1}). \tag{18}$$

S represents the weight factor and should be in the range of $(0, 1)$. Additionally, U denotes a vector of conserved variables, $\varphi_{i+1/2} = k.\,(\max \varphi_{i+1}, \varphi_i)$ and $\varphi_{i-1/2} = k.\,(\max \varphi_{i-1}, \varphi_i)$ with k representing the viscosity parameter. Table 1 presents the variables used for the analysis in this context.

4.1 Test I: Rarefaction Wave with Free-Flow Traffic

Free-flow traffic refers to a low-density regime in which vehicles travel independently of one another at their desired speed, without significant interaction effects. This occurs when the traffic density is low, indicating fewer vehicles on the road. In the first example, a discontinuity in the initial density profile can be observed, as described by the initial conditions presented in Equation (19). The discontinuity is located at 6000 m. The free-flow traffic is dominant upstream and downstream of the discontinuity, although the upstream density is considerably higher than downstream. Consequently, rarefaction waves are anticipated to propagate in both upstream and downstream directions.

$$\rho\,(x,0) = \begin{cases} 0.46\rho_m & x < \frac{L}{2}, \\ 0.1\rho_m & x > \frac{L}{2}, \end{cases} \tag{19}$$

$$v\,(x,0) = \nu_e\,(\rho\,(x,0))\,.$$

Table 1: Numerical and physical parameters used for AR and ARZ models [16]

Model	Parameter	Value
AR	Critical density (ρ_{Cr})	0.04 veh/m
	C_0^2	80 m^2/s^2
	ψ	31.94
	γ	0.5
ARZ	Critical density (ρ_{Cr})	0.075 veh/m
Both	Length of road (L)	12000 m
	Maximum speed $(v_{\max})$	30 m/s
	Maximum density (ρ_m)	0.15 veh/m
	S	0.1
	k	0.25
	Δt	1
	Δx	31.7 m
	$\max(\lambda_1, \lambda_2)$	30 m/s
	Δt (Reference solution)	0.625
	Δx (Reference solution)	1.8

Figure 1 compares the density profiles of AR and ARZ models with the results of the IWP-HLLE approach at times $t = 50s$ and $t = 150$. As can be observed in profiles (1-a) and (1-b), the IWP-HLLE method has successfully reduced numerical oscillations arising from discontinuities at $x = 6000m$. Additionally, the IWP-HLLE method in profiles (1-c) and (1-d) has effectively reduced oscillations similar to the other two methods for solving the ARZ model. The Root Mean Squared Error (RMSE) [11], defined in Equation (20), serves as the statistical metric utilized in this analysis.

$$RMSE = \sqrt{\frac{(y_i - y)^2}{n}}, \tag{20}$$

where y_i represents the value obtained from the IWP-HLLE method, y is the value from the reference method in the same section, and n shows the number of points whose values are taken. According to the RMSE values calculated in Table 2, the proposed method has demonstrated lower numerical dispersion than the other two methods at times $t = 50s$ and $t = 150s$ for the AR model, and at $t = 50s$ for the ARZ model.

Figure 2 illustrates the spatiotemporal density variation in solving the AR and ARZ models for test I. As can be observed in profiles (2: a-d), the density level in AV and CD methods has exhibited significant oscillations at $x = 6000m$. On the other hand, profiles (2e) and (2-f) have shown the capability of the IWP-HLLE approach in decreasing these oscillations.

4.2 Test II: Rarefaction Wave in Congested Traffic

In this test, a congestion state is predominant upstream and downstream of the discontinuity located at $x = 6000m$. The density decreases downstream based on Equation (21). As time progresses, rarefaction waves propagate in both the upstream and downstream directions. The propagation of these waves is depicted in Figures 3 and 4, and the errors are calculated in Table 3.

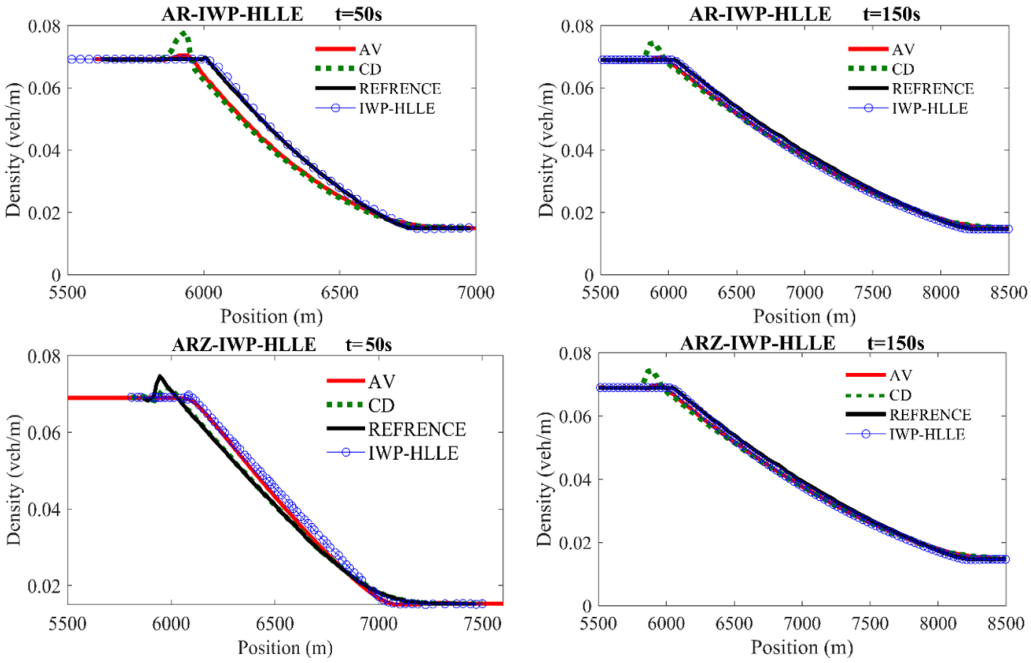

Figure 1: Rarefaction wave with free-flow traffic: Density profiles obtained using AV [16], CD [16]], and IWP–HLLE methods for the AR and ARZ models at $t = 50s$ and $t = 150s$. Simulations are performed on a uniform grid with $\Delta x = 31.7m$, $CFL = 0.9$, and MC limiter for the IWP–HLLE scheme.

Table 2: Rarefaction wave with free-flow traffic: RMSE calculated values between the results of AV [16], CD [16], and IWP-HLLE methods ($\Delta x = 31.7$ m) in comparison with the fine-grid reference solution ($\Delta x = 1.8$ m) [16] for AR and ARZ models at times $t = 50$s and $t = 150$s.

Test	Model	Time (s)	Method	RMSE (m)
Test I	AR	50	AV	2.49×10^{-6}
			CD	8.78×10^{-6}
			IWP-HLLE	1.06×10^{-6}
		150	AV	5.44×10^{-6}
			CD	8.29×10^{-6}
			IWP-HLLE	4.27×10^{-6}
	ARZ	50	AV	1.03×10^{-5}
			CD	1.02×10^{-5}
			IWP-HLLE	9.95×10^{-6}
		150	AV	4.29×10^{-6}
			CD	8.30×10^{-6}
			IWP-HLLE	4.32×10^{-6}

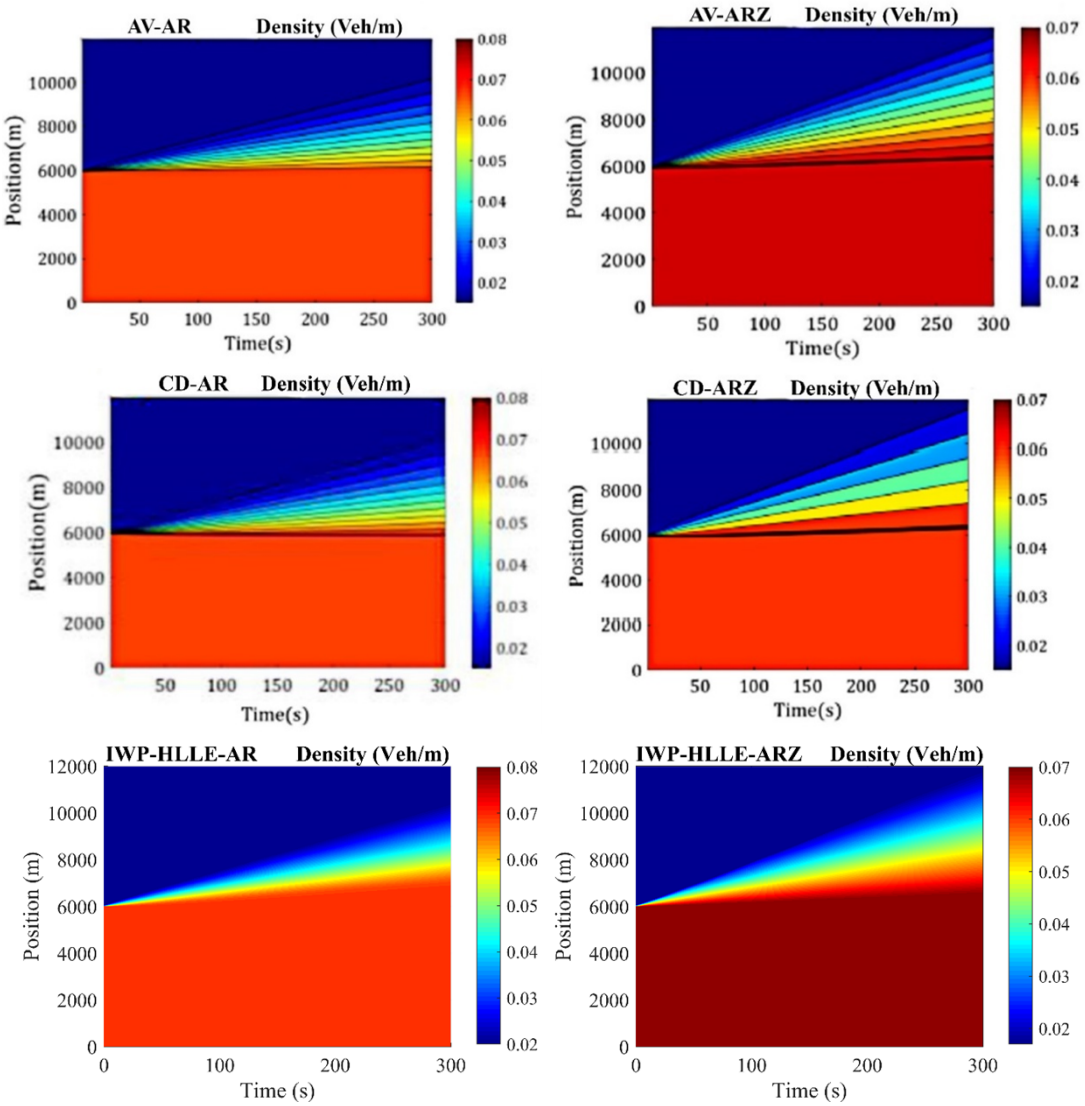

Figure 2: Spatiotemporal evolution of local densities for the AR and ARZ models obtained using AV [16], CD [16], and IWP–HLLE methods. The simulations use $\Delta x = 31.7m$, Δt determined by $CFL = 0.9$, and a total simulation time of $150s$.

$$\rho\left(x,0\right) = \begin{cases} 0.9\rho_m, & x < \frac{L}{2}, \\ 0.55\rho_m, & x > \frac{L}{2}, \end{cases} \tag{21}$$

$$v\left(x,0\right) = \nu_e\left(\rho\left(x,0\right)\right).$$

As shown in Figures 3 and 4, the proposed method has significantly outperformed the other methods in mitigating numerical oscillations near the discontinuity. In particular, the CD and AV smoothing methods have shown the highest level of oscillations compared to the reference method near the discontinuity in both the AR and ARZ models at $t = 50s$, as depicted in profiles (3-a) and (3-c).

As calculated in Table 3, the IWP-HLLE has the lowest values of RMSE compared to the smoothing method. It can be seen in Figure 4 that the density fluctuations at $x = 6000m$ have been decreased using the IWP-HLLE method compared to the AV and CD methods.

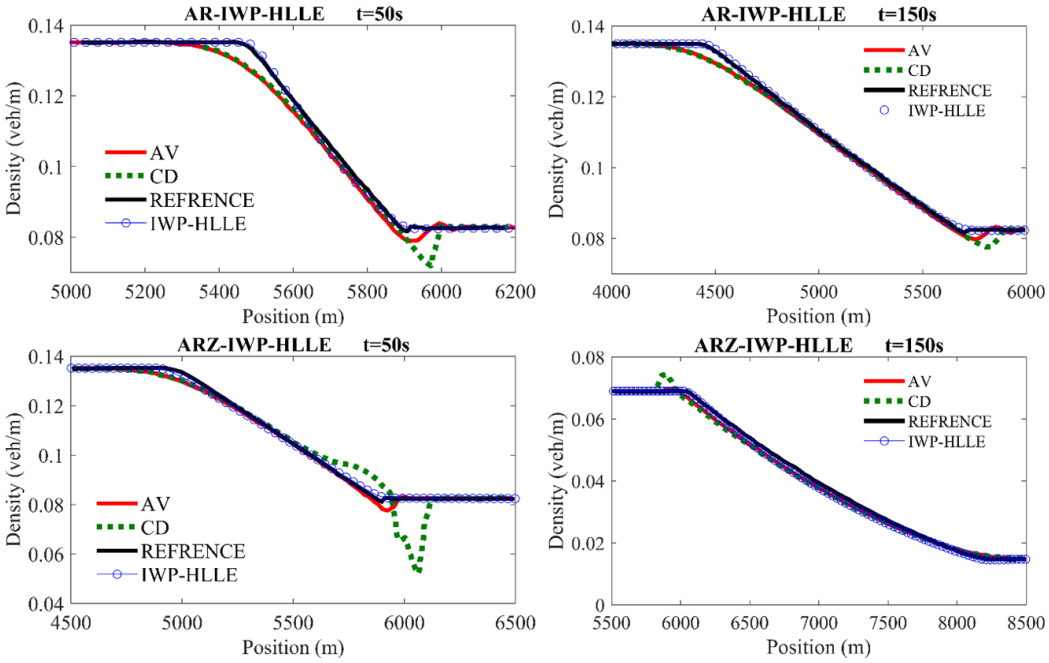

Figure 3: Rarefaction wave in congested traffic: Density profiles obtained using AV [16], CD [16], and IWP–HLLE methods for the AR and ARZ models at $t = 50$ s and $t = 150s$. Simulations are performed on a uniform grid with $\delta x = 31.7$ m, $CFL = 0.9$, and MC limiter for the IWP–HLLE scheme.

Table 3: Rarefaction wave in congested traffic: RMSE calculated values between the results of AV [16], CD [16], and IWP-HLLE methods ($\Delta x = 31.7m$) in comparison with the fine-grid reference solution ($\Delta x = 1.8m$) [16] for AR and ARZ models at times $t = 50s$ and $t = 150s$.

Test	Model	Time (s)	Method	RMSE (m)
Test II	AR	50	AV	2.31×10^{-6}
			CD	1.57×10^{-4}
			IWP-HLLE	1.28×10^{-5}
		150	AV	1.69×10^{-5}
			CD	3.15×10^{-5}
			IWP-HLLE	4.26×10^{-6}
	ARZ	50	AV	2.59×10^{-5}
			CD	3.90×10^{-4}
			IWP-HLLE	1.36×10^{-5}
		150	AV	5.24×10^{-6}
			CD	7.95×10^{-5}
			IWP-HLLE	7.18×10^{-7}

4.3 Test III: Queue Dissolution

This test examines the queue dissolution in a uniform state of flow. Equation (22) presents the density values at different path sections. Free flow conditions dominate the initial and final one-third of the path. There is congestion in the rest of the path. Therefore, two discontinuities in the density-position profile and two Riemann problems

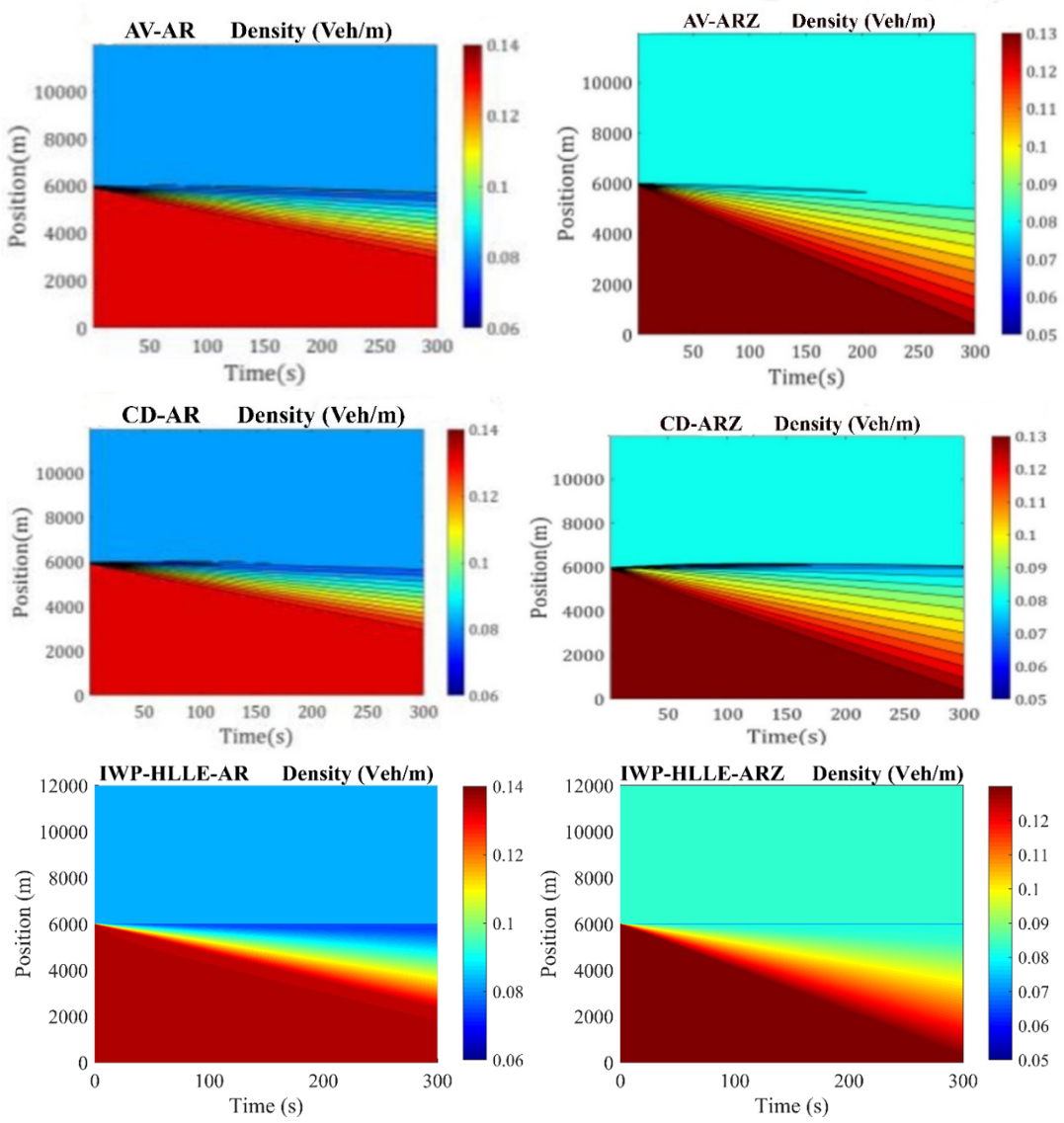

Figure 4: Rarefaction wave in congested traffic: Spatiotemporal evolution of local densities for the AR and ARZ models obtained using AV [16], CD [16], and IWP–HLLE methods. The simulations use $\Delta x = 31.7m$, Δt determined by $CFL = 0.9$, and a total simulation time of $150s$.

exist concurrently in this test. At the first discontinuity, shock waves propagate in the upstream direction. At the second discontinuity, rarefaction waves develop and propagate in both the upstream and downstream directions over time.

$$\rho(x,0) = \begin{cases} 0.1\rho_m, & x < \frac{L}{3}, \\ \rho_m, & \frac{L}{3} < x < \frac{2L}{3}, \\ 0.1\rho_m, & x > \frac{2L}{3} \end{cases} \tag{22}$$

$$v(x,0) = \nu_e(\rho(x,0)).$$

Figure 5 shows density profiles for queue dissolution at two-time intervals, i.e., $t = 50s$ and $t = 150s$. It is evident from Figure 5 that the IWP-HLLE method has successfully reduced oscillations at the discontinuities

compared to the CD method. Furthermore, comparing the proposed method with the AV approach has demonstrated a better reduction of oscillations at $t = 50s$ for the ARZ model. Table 4 calculates the statistical results of comparing AV, CD, and IWP-HLLE approaches with the reference method.

The results indicate that the IWP-HLLE method is capable of handling the initial value discontinuities and reducing numerical oscillations at $x = 4000m$ and $x = 8000m$. In addition, this method has exhibited superior performance compared to the AV method at $t = 150s$ for the AR model and at $t = 50s$ for the ARZ model (with RMSE values of $1.42 \times 10^{-5}m$ and $4.69 \times 10^{-4}m$, respectively). Figure 6 illustrates the spatiotemporal changes in density for both the AR and ARZ models in this test. As can be observed, the level of numerical oscillations at discontinuities is nearly similar in all three methods. Overall, the IWP-HLLE method has effectively reduced numerical oscillations at the discontinuities, provided better solutions than the CD method, and outperformed the AV method at specific times for both models.

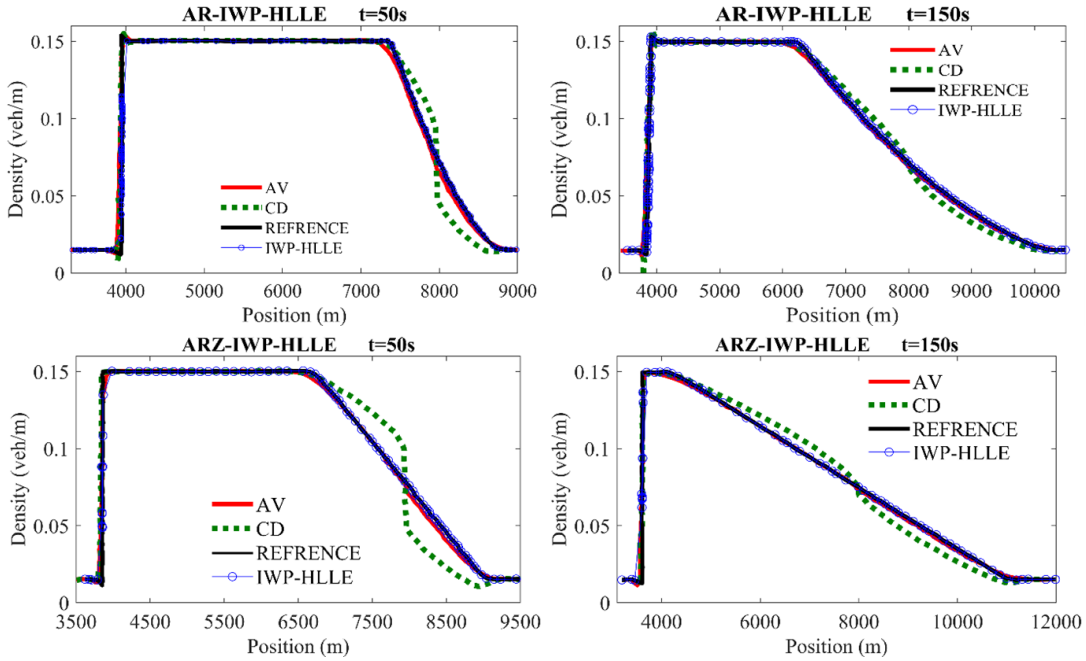

Figure 5: Queue dissolution: Density profiles computed using AV [16], CD [16], and IWP–HLLE methods at $t = 50s$ and $t = 150s$. All numerical schemes use the same grid resolution ($\Delta x = 31.7m$) and $CFL = 0.9$. The reference solution is obtained on a refined grid with $\Delta x = 1.8m$.

4.4 Test IV: Congested Traffic Flow with Non-Equilibrium Velocity and Uniform Density

The initial traffic conditions in this test are non-equilibrium, and the velocities are non-uniform, leading to the formation of contact discontinuities:

$$\nu\,(x,0) = \begin{cases} v_e(\rho(x,0)) + 5, & x < \frac{L}{3}, \\ v_e\left(\rho\,(x,0)\right), & \frac{L}{3} < x < \frac{2L}{3}, \\ v_e(\rho(x,0)) + 5, & x > \frac{2L}{3} \end{cases} \tag{23}$$

$$\rho\,(x,0) = 0.75\rho_m.$$

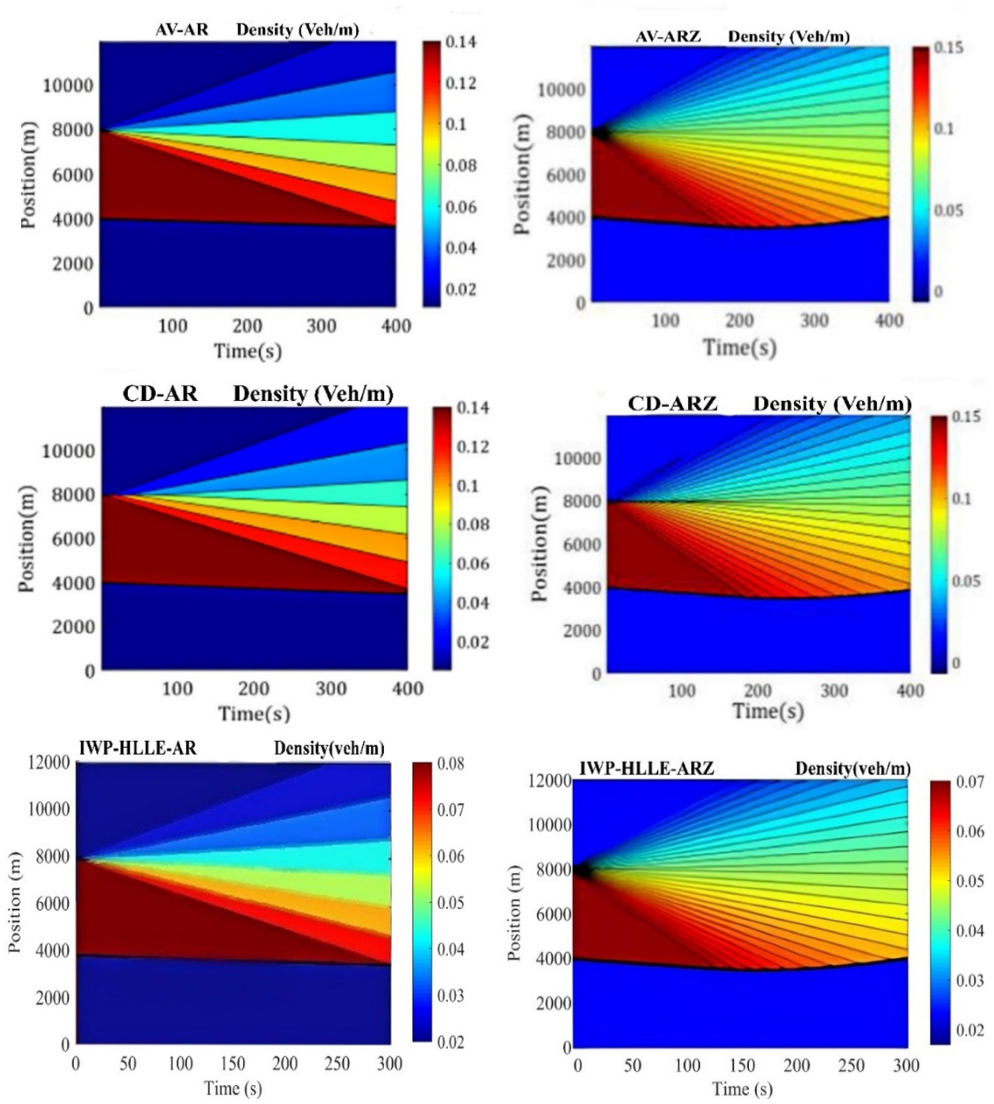

Figure 6: Queue dissolution: Spatiotemporal evolution of local densities for the AR and ARZ models obtained using AV [16], CD [16]], and IWP–HLLE methods. The simulations use $\Delta x = 31.7m$, Δt determined by $CFL = 0.9$, and a total simulation time of $150s$.

Table 4: Queue dissolution: RMSE calculated values between the results of AV [16], CD [16], and IWP-HLLE methods ($\Delta x = 31.7m$) in comparison with the fine-grid reference solution ($\Delta x = 1.8m$) [16] for AR and ARZ models at times $t = 50s$ and $t = 150s$.

Test	Model	Time (s)	Method	RMSE (m)
Test III	AR	50	AV	2.32×10^{-4}
			CD	3.59×10^{-4}
			IWP-HLLE	2.84×10^{-4}
		150	AV	1.19×10^{-4}
			CD	4.18×10^{-4}
			IWP-HLLE	1.42×10^{-5}
	ARZ	50	AV	6.81×10^{-4}
			CD	8.18×10^{-4}
			IWP-HLLE	4.69×10^{-4}
		150	AV	7.85×10^{-5}
			CD	9.81×10^{-4}
			IWP-HLLE	5.70×10^{-4}

As depicted in Figures 7 and 8, along with Table 5, numerical oscillations are not evident in the results obtained from the IWP-HLLE method. However, there are specific areas where oscillations can be observed using the other two methods. For instance, the AR model has demonstrated significant oscillations between the $x = 8000m$ and $x = 8700m$ at $t = 50s$. The RMSE for the AR model using the IWP-HLLE method has been calculated equal to 1.79×10^{-4} at $t = 150s$, showing better performance than the other two methods. However, this value is higher than the CD method at earlier times ($t = 50s$). The RMSE values for the ARZ model have proved the better performance of the proposed IWP-HLLE approach. As shown in Figures 7 and 8, despite the significant reduction in oscillatory behavior achieved by the proposed scheme compared to classical techniques, some residual oscillations may persist under non-equilibrium conditions. These oscillations arise from the nonlinear coupling of characteristic fields. However, they do not compromise the solution's accuracy or stability, since the error amplification factor diminishes over time.

The computed solutions are physically meaningful and consistent with observed traffic dynamics. Shock waves represent abrupt vehicle deceleration, typically associated with sudden congestion onset or bottleneck activation. Rarefaction waves characterize the gradual acceleration of vehicles in low-density regions as traffic spreads. Contact discontinuities describe transitions between flow regions of equal density but different velocities, arising from non-equilibrium initial conditions.

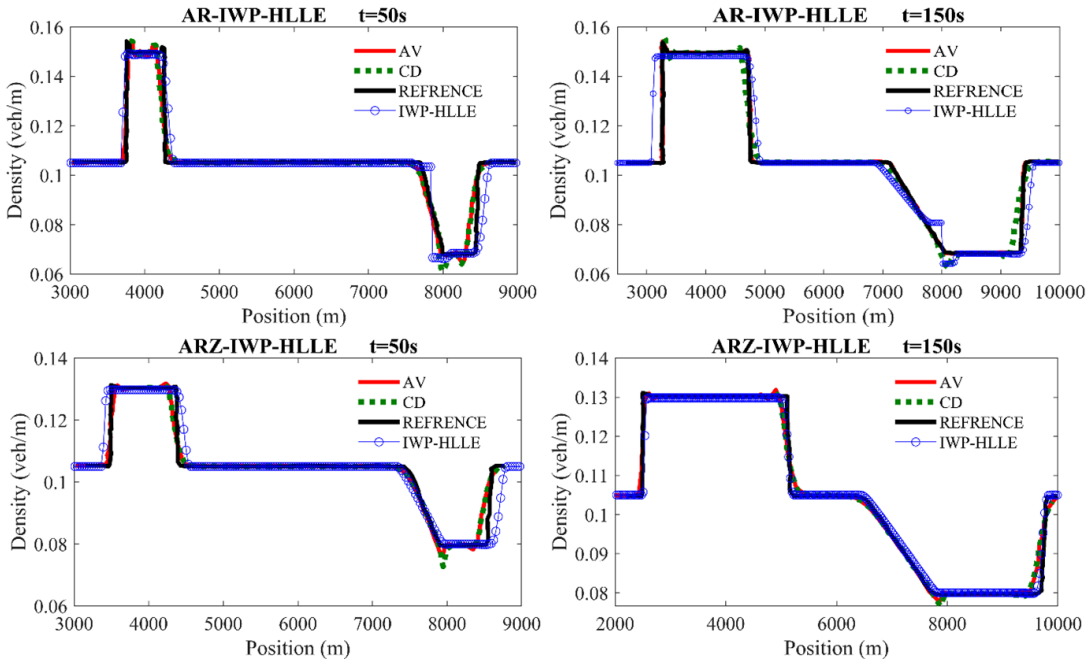

Figure 7: Congested traffic flow with non-equilibrium velocity and uniform density: Density profiles for the AR and ARZ models at $t = 50s$ and $t = 150s$, computed with $\Delta x = 31.8m$, $CFL = 0.9$, and MC limiter for the IWP–HLLE scheme.

Table 5: Congested traffic flow with non-equilibrium velocity and uniform density: RMSE calculated values between the results of AV [16], CD [16], and IWP-HLLE methods ($\Delta x = 31.7m$) in comparison with the fine-grid reference solution ($\Delta x = 1.8m$) [16] for AR and ARZ models at times $t = 50s$ and $t = 150s$.

Test	Model	Time (s)	Method	RMSE (m)
Test V	AR	50	AV	9.21×10^{-5}
			CD	8.08×10^{-4}
			IWP-HLLE	5.14×10^{-4}
		150	AV	2.52×10^{-4}
			CD	7.46×10^{-4}
			IWP-HLLE	1.79×10^{-4}
	ARZ	50	AV	5.06×10^{-6}
			CD	2.33×10^{-4}
			IWP-HLLE	1.59×10^{-4}
		150	AV	2.08×10^{-5}
			CD	2.72×10^{-4}
			IWP-HLLE	7.81×10^{-5}

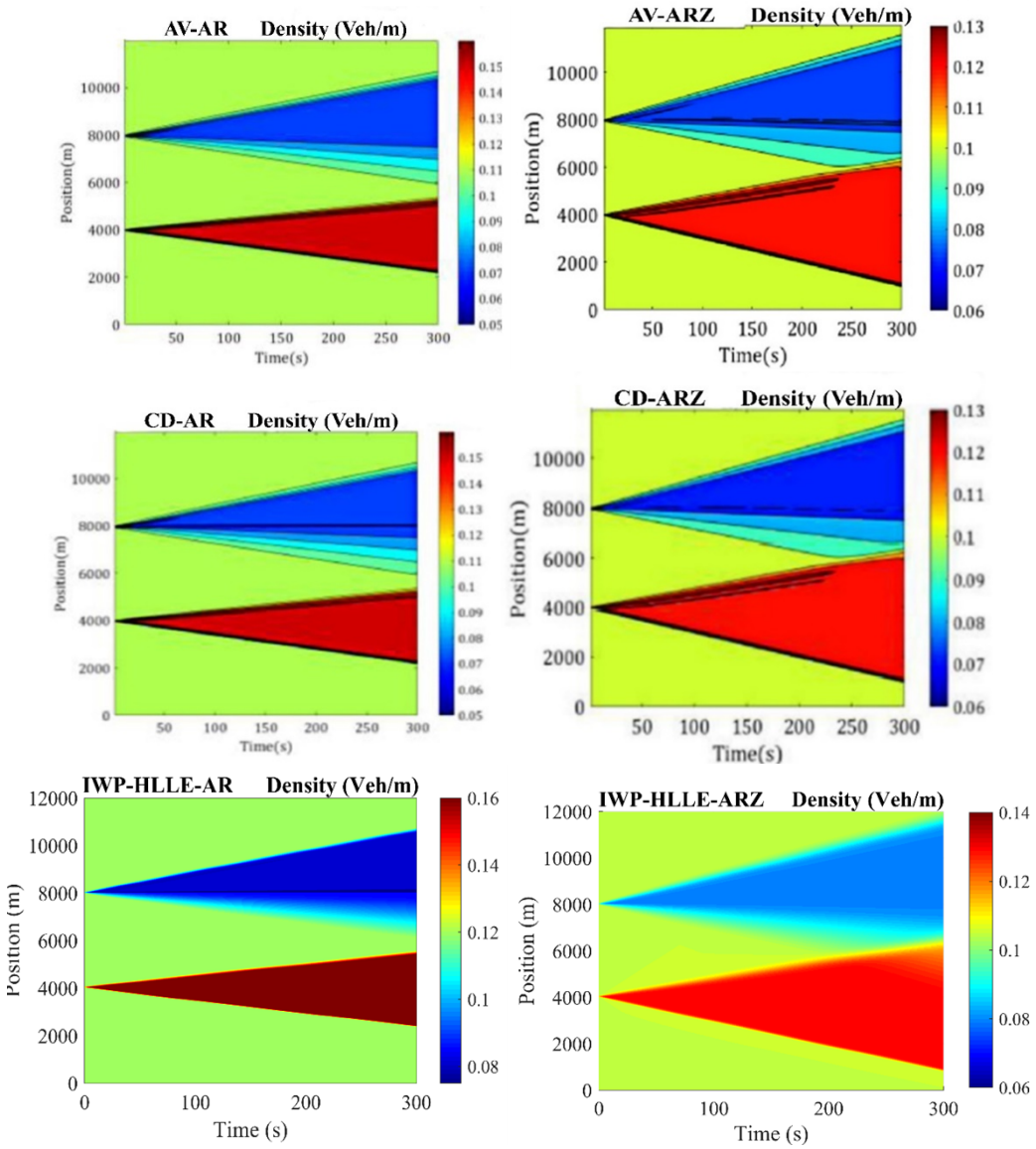

Figure 8: Congested traffic flow with non-equilibrium velocity and uniform density: Spatiotemporal evolution of local densities for the AR and ARZ models obtained using AV [16], CD [16], and IWP–HLLE methods. The simulations use $\Delta x = 31.7m$, Δt determined by $CFL = 0.9$, and a total simulation time of $150s$.

5 Conclusions

This study presented the IWP-HLLE approach for the numerical solution of homogeneous second-order Aw-Rascle-type traffic flow equations. General algorithmic formulations were derived for both the Aw-Rascle (AR) and Aw-Rascle-Zhang (ARZ) models. To evaluate the proposed method, four benchmark tests involving shock waves, rarefaction waves, and contact discontinuities were solved for homogeneous long-road geometries ($L = 12000\,\text{m}$), and the results were compared against the standard MacCormack scheme combined with artificial viscosity (AV) and central differencing (CD) smoothing techniques. Spatiotemporal and density-position profiles were examined at $t = 50\,\text{s}$ and $t = 150\,\text{s}$.

The IWP-HLLE method accurately captured the formation and propagation of rarefaction waves, contact discontinuities, and shocks by properly coordinating wave propagation directions. Unlike the CD and AV methods, which exhibited spurious oscillations near discontinuities, the proposed approach remained oscillation-free at wave fronts in all test cases. The Monotonized Central (MC) limiter proved highly effective in controlling numerical dispersion. Quantitative assessment via RMSE confirmed that the IWP-HLLE method outperformed both smoothing techniques for the AR model in tests I, II, and III, and for the ARZ model in tests I and II. For example, RMSE values for the AR model in test I were 1.06×10^{-5} and 4.27×10^{-6} at $t = 50\,\text{s}$ and $t = 150\,\text{s}$, respectively, corresponding to reductions of 57% and 21.5% relative to the AV method. For the AR model in test IV, the IWP-HLLE method produced superior results only at $t = 150\,\text{s}$, with residual oscillations observed under non-equilibrium velocity conditions, arising from the nonlinear coupling of characteristic fields. Nevertheless, the error amplification factor diminished over time, confirming the long-term stability of the method.

Recommendations for Future Research. Based on the findings and limitations identified in this study, the following directions are recommended for future investigations:

- *Extension to two-dimensional frameworks:* The current formulation is restricted to one-dimensional road segments. Extending the IWP-HLLE approach to two-dimensional networks would enable the simulation of intersections, lane-changing dynamics, and multi-route traffic systems, significantly broadening its practical applicability.
- *Integration with higher-order schemes:* Although the present method achieves second-order accuracy in smooth regions, coupling the IWP-HLLE approach with higher-order reconstruction techniques such as WENO or MUSCL could further reduce numerical diffusion near sharp gradients while maintaining the positivity properties of the proposed wave-speed strategy.
- *Treatment of non-homogeneous models:* The proposed framework is currently limited to homogeneous models. Incorporating source terms, such as relaxation-based acceleration terms found in Payne-Whitham-type models, would extend the method's applicability to a broader class of non-homogeneous second-order traffic flow models.
- *Non-equilibrium conditions and flux limiters:* The residual oscillations observed in test IV under non-equilibrium velocity conditions suggest that alternative flux limiters or adaptive regularization strategies should be investigated to fully suppress spurious behavior in strongly non-equilibrium regimes.

Declarations

Availability of Supporting Data

All data generated or analyzed during this study are included in this published paper.

Funding

The authors conducted this research without any funding, grants, or support.

Conflict of Interest

The authors declare that they have no known competing financial interests or personal relationships that could have influenced the work reported in this paper.

Author Contributions

Alireza Ezzati: Conceptualization; Methodology; Mathematical Modeling; Visualization; Writing-Original Draft. **Mahdi Mollazadeh**: Validation; Formal analysis; Overall Guidance. **Sadegh Moodi**: Conceptualization; Mathematical Modeling; Overall Guidance; Writing-review and editing. **Morteza Araghi**: Conceptualization; Mathematical Modeling; Overall Guidance; Project administration; Writing-review and editing. **Hossein Mahdizadeh**: Conceptualization; Resources; Overall Guidance.

Artificial Intelligence Statement

Artificial intelligence (AI) tools, including large language models, were used solely for language editing and improving readability. AI tools were not used for generating ideas, performing analyses, interpreting results, or writing the scientific content. All scientific conclusions and intellectual contributions were made exclusively by the authors.

Publisher's Note

The publisher remains neutral regarding jurisdictional claims in published maps and institutional affiliations.

References

[1] Araghi, M., Mahdizadeh, H., Moodi, S. (2021). "Numerical modelling of macroscopic traffic flow based on driver physiological response using a modified wave propagation algorithm". *Journal of Decisions and Operations Research*, 6(3), 350–364. https://doi.org/10.22105/dmor.2021.271141.1313

[2] Araghi, M., Mahdizadeh, S., Mahdizadeh, H., Moodi, S. (2021). "A modified flux-wave formula for the solution of second-order macroscopic traffic flow models". *Nonlinear Dynamics*, 106(4), 3507–3520. https://doi.org/10.1007/s11071-021-06935-w

[3] Aw, A., Rascle, M. (2000). "Resurrection of second order models of traffic flow". *SIAM Journal on Applied Mathematics*, 60(3), 916–938. https://doi.org/10.1137/S0036139997332099

[4] Dabiri, A., Kulcsár, B. (2015). "Freeway traffic incident reconstruction – A bi-parameter approach". *Transportation Research Part C: Emerging Technologies*, 58, 585–597. https://doi.org/10.1016/j.trc.2015.03.038

[5] Delis, A.I., Nikolos, I.K., Papageorgiou, M. (2014). "High-resolution numerical relaxation approximations to second-order macroscopic traffic flow models". *Transportation Research Part C: Emerging Technologies*, 44, 318–349. https://doi.org/10.1016/j.trc.2014.04.004

[6] Delis, A.I., Nikolos, I.K., Papageorgiou, M. (2015). "Macroscopic traffic flow modeling with adaptive cruise control: Development and numerical solution". *Computers & Mathematics with Applications*, 70(8), 1921–1947. https://doi.org/10.1016/j.camwa.2015.08.002

[7] Einfeldt, B. (1988). "On Godunov-type methods for gas dynamics". *SIAM Journal on Numerical Analysis*, 25(2), 294–318. https://doi.org/10.1137/0725021

[8] Kerner, B. S., Konhäuser, P. (1994). "Structure and parameters of clusters in traffic flow". *Physical Review E*, 50(1), 54–83. https://doi.org/10.1103/PhysRevE.50.54

[9] Khan, Z.H., Gulliver, T.A., Nasir, H., Rehman, A., Shahzada, K. (2019). "A macroscopic traffic model based on driver physiological response". *Journal of Engineering Mathematics*, 115(1), 21–41. https://doi.org/10.1007/s10665-019-09990-w

[10] Lebacque, J.-P., Mammar, S., Haj-Salem, H. (2007). "The Aw–Rascle and Zhang's model: Vacuum problems, existence and regularity of the solutions of the Riemann problem". *Transportation Research Part B: Methodological*, 41(7), 710–721. https://doi.org/10.1016/j.trb.2006.11.005

[11] LeVeque, R.J. (2002). "Finite volume methods for hyperbolic problems". *Cambridge University Press*. https://doi.org/10.1017/CBO9780511791253

[12] Mahdizadeh, H., Sharifi, S., Omidvar, P. (2018). "On the approximation of two-dimensional transient pipe flow using a modified wave propagation algorithm". *Journal of Fluids Engineering*, 140(7). https://doi.org/10.1115/1.4039248

[13] Mahdizadeh, H., Stansby, P.k., Rogers, B.D. (2012). "Flood wave modeling based on a two-dimensional modified wave propagation algorithm coupled to a full-pipe network solver". *Journal of Hydraulic Engineering*, 138(3), 247–259. https://doi.org/10.1061/(ASCE)HY.1943-7900.0000515

[14] Mohamed, K., Abdelrahman, M.A.E. (2023). "The NHRS scheme for the two models of traffic flow". *Computational and Applied Mathematics*, 42(1), 53. https://doi.org/10.1007/s40314-022-02172-y

[15] Mohammadian, S., Moghaddam, A.M., Sahaf, A. (2021). "On the performance of HLL, HLLC, and Rusanov solvers for hyperbolic traffic models". *Computers & Fluids*, 231, 105161. https://doi.org/10.1016/j.compfluid.2021.105161

[16] Mohammadian, S., van Wageningen-Kessels, F. (2018). "Improved numerical method for Aw-Rascle type continuum traffic flow models". *Transportation Research Record*, 2672(20), 262–276. https://doi.org/10.1177/0361198118784402

[17] Payne, H. (1971). "Mathematical models of public systems". *Simulation Council Proceedings Series*, 1, 51–61.

[18] Rastegar Moghadam Najafzadeh, M., Araghi, M., Moodi, S., Mollazadeh, M., Mahdizadeh, H. (2025). "An improved flux wave-HLLE approach for the solution of traffic flow models based on transition velocities". *AUT Journal of Civil Engineering*, 9(2), 159–170. https://doi.org/10.22060/ajce.2025.23594.5887

[19] Smoller, J. (2012). "Shock waves and reaction–diffusion equations". *Springer New York*. https://doi.org/10.1007/978-1-4612-0873-0

[20] Treiber, M., Kesting, A. (2013). "Traffic flow dynamics: Data, models and simulation". *Springer Berlin Heidelberg*. https://doi.org/10.1007/978-3-642-32460-4

[21] van Wageningen-Kessels, F., van Lint, H., Vuik, K., Hoogendoorn, S. (2015). "Genealogy of traffic flow models". *EURO Journal on Transportation and Logistics*, 4(4), 445–73. https://doi.org/10.1007/s13676-014-0045-5

[22] Witham, GB. (1974). "Linear and non-linear waves". *John Wiley & Sons, New York*. https://doi.org/10.1002/9781118032954

[23] Zhang, H.M. (2001). "New perspectives on continuum traffic flow models". *Networks and Spatial Economics*, 1(1), 9–33. https://doi.org/10.1023/A:1011539112438

[24] Zhang, H.M. (2002). "A non-equilibrium traffic model devoid of gas-like behavior". *Transportation Research Part B: Methodological*, 36(3), 275–90. https://doi.org/10.1016/S0191-2615(00)00050-3

Authors Bio-sketches

Alireza Ezzati received his MSc in Water and Hydraulic Structures from the University of Birjand, Iran. His research focuses on macroscopic traffic flow modeling using wave propagation and finite-volume methods. He applies conservation-law formulations and numerical schemes originally developed in fluid mechanics to simulate hyperbolic systems and analyze discontinuous traffic dynamics.

Mahdi Mollazadeh is an Assistant Professor of Civil Engineering at the University of Birjand, Iran. He holds a PhD in Hydraulic Structures and works in hydraulic modeling and computational simulation of complex flow systems. His research interests include stepped spillways, skimming flow regimes, and advanced numerical techniques in hydraulic engineering.

Sadegh Moodi is an Assistant Professor at Birjand University of Technology, Iran. His primary expertise is in water engineering and hydraulic structures, with emphasis on numerical modeling of hydraulic flows and conservation-law systems. He also applies related computational and wave-propagation methods to interdisciplinary problems, including macroscopic traffic flow modeling.

Morteza Araghi is an Assistant Professor at the University of Birjand, Iran. His research focuses on macroscopic traffic flow theory and numerical methods for hyperbolic partial differential equations. He works on wave propagation algorithms, approximate Riemann solvers, and stable shock-capturing schemes for second-order traffic models.

Corresponding author: Email: m.araghi@birjand.ac.ir

Hossein Mahdizadeh is an Associate Professor at the University of Birjand, Iran. His main research area is hydraulic engineering and numerical modeling of nonlinear flow systems. Recently, he has been actively developing particle-based computational methods, particularly Smoothed Particle Hydrodynamics (SPH), with emphasis on stability, accuracy, and high-fidelity simulation of free-surface flows.